Surfactant-induced protein unfolding as studied by small-angle neutron scattering and dynamic light scattering

2007 J. Phys.: Condens. Matter 19 326102

(http://iopscience.iop.org/0953-8984/19/32/326102)

IOP PUBLISHING JOURNAL OF PHYSICS: CONDENSED MATTER

J. Phys.: Condens. Matter **19** (2007) 326102 (12pp) doi:10.1088/0953-8984/19/32/326102

Surfactant-induced protein unfolding as studied by small-angle neutron scattering and dynamic light scattering

S Chodankar[1], V K Aswal[1], J Kohlbrecher[2], R Vavrin[2] and A G Wagh[1]

[1] Solid State Physics Division, Bhabha Atomic Research Centre, Mumbai-400 085, India
[2] Laboratory for Neutron Scattering, ETH Zurich and Paul Scherrer Institut, CH-5232 Villigen PSI, Switzerland

E-mail: vkaswal@barc.gov.in

Received 16 April 2007, in final form 30 May 2007
Published 13 July 2007
Online at stacks.iop.org/JPhysCM/19/326102

Abstract

The structural changes of protein bovine serum albumin (BSA) during its unfolding on the addition of anionic surfactant sodium dodecyl sulfate (SDS) have been studied using small-angle neutron scattering (SANS) and dynamic light scattering (DLS). It is observed that at small surfactant concentrations, individual surfactant molecules bind to the protein, increasing the size of the protein. On the other hand, surfactant molecules at higher concentrations aggregate to form micelle-like clusters along the unfolded polypeptide chains of the protein. SANS data indicates the formation of a fractal structure representing a necklace model of micelle-like clusters randomly distributed along the polypeptide chain. The overall size of the complex increases and the fractal dimension decreases on increasing the surfactant concentration. The size of the micelle-like clusters does not show any change, while the number of such micelle-like clusters in protein–surfactant complexes increases with the surfactant concentration. The conformation of the unfolded protein has been determined directly using contrast variation SANS measurements by contrast matching the surfactant to the medium. It is found that the protein acquires a random coil Gaussian conformation on unfolding, with its radius of gyration increasing with an increase in surfactant concentration. The results of DLS measurements are found to be in good agreement with those obtained using SANS.

1. Introduction

The bulk properties of any colloidal system are mainly determined by the nature and interactions amongst the various kinds of constituent particles [1, 2]. Mixtures of protein

and surfactant complexes are one kind of such colloidal systems that find their usefulness in a variety of pharmaceutical, cosmetic and food products [3–5]. Ionic surfactants and proteins share the property of both charged groups and hydrophobic portions. It is believed that surfactant molecules at low concentrations undergo electrostatic binding to the protein, whereas, above critical aggregation concentration, hydrophobic interaction among surfactant molecules takes over the binding process [6–9]. At higher surfactant concentrations, the binding of surfactants to the protein macromolecules leads to their denaturation, which is considered to be surfactant-induced unfolding of the protein [10–14]. Understanding the behavior of such protein–surfactant complexes is of vital interest and allows us to gain insight into the binding mechanism between the two components and its effect on the protein structure and function in the complex [15–17].

Various techniques, such as circular dichroism (CD) [18, 19], nuclear magnetic resonance (NMR) [20], microcalorimetry [21], light scattering [22] and small-angle scattering [23–29], have been used to understand the mechanism of unfolding of protein on addition of surfactant. The results of these techniques lead to the proposition of several models about the interaction of surfactants with protein, such as a rod-like model, a flexible helix model and a necklace model. It is found that, out of these models, the necklace model is the most accepted model for the understanding of the interaction of the two components in their complex formation [30]. The necklace model was originally based on results from free boundary electrophoresis [31], and data from other techniques, such as small-angle neutron scattering (SANS) [23] and NMR [32], also supports this model.

SANS has been used to evaluate the protein–surfactant complex as a fractal structure based on the necklace model that comprises micelle-like clusters randomly distributed along the polypeptide chain of the unfolded protein [23]. This technique has been quite useful for yielding detailed information, such as the fractal dimension of the protein–surfactant complex characterizing the distribution of micelle-like clusters bound to the protein, the extent of the complex and the average size of the micelle-like clusters in the complex. Most of the SANS studies have been performed at high surfactant concentrations [23–25]. These studies show that the fractal dimension decreases and the overall size of the complex increases with an increase in surfactant concentration. On the other hand, small-angle x-ray scattering (SAXS) measurements have been performed on these systems over wide surfactant concentrations [26–29]. The SAXS data shows, in contrast to SANS, that the fractal dimension and the overall size of the complex do not change as the surfactant concentration is increased. Due to the fact that x-ray scattering occurs from the electron cloud of the atom, the magnitude of scattering for any component in SAXS increases with the increase in the atomic number (Z). Since the value of average Z in the head group (SO_4^-) region of SDS micelles is much higher than those of the core and the solvent, scattering in the case of SAXS is strongly dominated by the shell-like structure of head-groups of the micelles. As a result of this limitation, SAXS data do not show any significant change in the functionality on varying the surfactant concentration in the complex [27, 28]. SANS has the advantage of being able to probe such structures composed of hydrogenous constituents and it also provides the opportunity of contrast variation to separate systematically the structure of individual constituents in the complex. In this paper, we report the structural changes of protein bovine serum albumin (BSA) on the addition of varying concentrations of anionic surfactant sodium dodecyl sulfate (SDS) as characterized by SANS and dynamic light scattering (DLS). SANS provides information on the shape and size of the complex. Furthermore, the unfolding mechanism is studied in more detail by using protonated and deuterated SDS to get different contrast conditions. DLS is a complimentary technique to SANS, which gives size information by measuring the diffusion coefficient of the complex.

2. Experiment

BSA protein (catalogue no. 05480) and SDS surfactant (catalogue no. 71727) were purchased from Fluka. Deuterated SDS (d-SDS) was purchased from Cambridge isotope laboratory. Samples for SANS experiments were prepared by dissolving a known amount of BSA and SDS in a buffer solution of D_2O. The use of D_2O as solvent instead of H_2O provides better contrast for hydrogenous components in neutron experiments. To contrast match the surfactant, d-SDS was used. The interparticle interactions in the system were minimized by preparing the samples in acetate buffer solution at pH 5.4, which is close to the isoelectric pH of BSA (4.9), and at a high ionic strength of 0.5 M NaCl. Small-angle neutron scattering experiments were performed on the SANS instrument at the Swiss Spallation Neutron Source SINQ, Paul Scherrer Institute, Switzerland [33]. The mean wavelength of the incident neutron beam was 6 Å, with a wavelength resolution of approximately 10%. The scattered neutrons were detected using a two-dimensional 96 cm × 96 cm detector. The experiments were performed at two sample-to-detector distances of 2 and 8 m, respectively, to cover the data in the wavevector transfer Q range of 0.007–0.25 $Å^{-1}$. The measurements were made for 1 wt% BSA in the presence of varying concentrations of SDS in the range 0 to 100 mM. The measured SANS data were corrected and normalized to a cross-sectional unit using standard procedures [34]. DLS measurements on the above samples were carried out using a commercial ALV/LSE-5003 light scattering instrument featuring a multiple tau digital correlator. The light source was a helium neon laser operated at 6328 Å and the measurements were performed at a scattering angle of 90°. The temperature during all the measurements was kept fixed at 30 °C.

3. Data analysis

3.1. Small-angle neutron scattering

In small-angle neutron scattering, one measures the coherent differential scattering cross-section ($d\Sigma/d\Omega$) per unit volume. For a system of mono-disperse interacting protein macromolecules, $d\Sigma/d\Omega(Q)$ can be expressed as [35]

$$\frac{d\Sigma}{d\Omega}(Q) = N_p V_p^2 (\rho_p - \rho_s)^2 \left[\left\langle F^2(Q)\right\rangle + \langle F(Q)\rangle^2 \left(S_p(Q) - 1\right)\right] + B \tag{1}$$

where N_p is the number density of the protein, ρ_p and ρ_s are the scattering length density of the protein and the solvent respectively, and V_p is the volume of the protein molecule. $F(Q)$ is the single-particle form factor and $S_p(Q)$ is the interparticle structure factor. B is a constant term that represents the incoherent scattering background, which is mainly due to hydrogen in the sample. The single-particle form factor has been calculated by treating the protein macromolecules as a prolate ellipsoidal. For such an ellipsoidal particle

$$\left\langle F^2(Q)\right\rangle = \int_0^1 \left[F(Q,\mu)^2\, d\mu\right] \tag{2}$$

$$\langle F(Q)\rangle^2 = \left[\int_0^1 F(Q,\mu)\, d\mu\right]^2 \tag{3}$$

$$F(Q,\mu) = \frac{3(\sin x - x\cos x)}{x^3} \tag{4}$$

$$x = Q\left[a^2\mu^2 + b^2(1-\mu^2)\right]^{1/2} \tag{5}$$

where a and b are, respectively, the semi-major and semi-minor axes of the ellipsoidal protein macromolecules and μ is the cosine of the angle between the directions of a and the wavevector transfer Q.

In general, charged colloidal systems such as protein solutions show a correlation peak in the SANS distribution. The peak arises because of the interparticle structure factor $S_p(Q)$ and indicates the presence of electrostatic interaction between the colloids. In the case of a low concentration of protein solution at high salt concentration and pH close to the isoelectric point of the protein, $S_p(Q)$ can be approximated to unity as the interparticle interactions are minimized.

The unfolding of proteins has been modeled using the necklace model of protein–surfactant complexes that assumes micelle-like clusters of surfactant randomly distributed along the unfolded polypeptide chain. The cross-section for such a system can be expressed as [23, 36]

$$\frac{d\Sigma}{d\Omega}(Q) = \frac{N_1^2}{N_p N}(b_m - V_m\rho_s)^2 P(Q) S_f(Q) + B \tag{6}$$

where N_1 is the number density of the total surfactant molecules in solution, V_m is the volume of the micelle, and N is the number of such micelles attached to a polypeptide chain. b_m represents the scattering length of the surfactant molecule. $P(Q)$ denotes the normalized intraparticle structure factor ($\langle F^2(Q)\rangle$) of a single micelle-like cluster, which for a spherical particle of radius R is given by

$$P(Q) = \left[\frac{3\{\sin(QR) - QR\cos(QR)\}}{(QR)^3}\right]^2 \tag{7}$$

$S_f(Q)$ has been calculated using a fractal structure for the necklace model of a protein–surfactant complex. The arrangement of micelle-like clusters is assumed to be a fractal packing of spheres. In this case, $S_f(Q)$ is given as [37]

$$S_f(Q) = 1 + \frac{1}{(QR)^D}\frac{D\Gamma(D-1)}{[1+(Q\xi)^{-2}]^{[(D-1)/2]}}\sin[(D-1)\tan^{-1}(Q\xi)] \tag{8}$$

where D is the fractal dimension of the micellar distribution in space and ξ is the correlation length that is a measure of the extent of unfolding of the polypeptide chain.

The dimensions of the protein macromolecule at low surfactant concentrations have been determined from the analysis. The semi-major axis (a) and the semi-minor axis ($b = c$) are the parameters in analyzing the SANS data. At higher surfactant concentrations the fractal dimension (D), characteristic length (ξ), number of micelles (N) and radius of micelles (R) are the fitted parameters to characterize the unfolding of protein. The calculated aggregation number of the micelle-like clusters in the complex is calculated by $n = N_1/(N_p N)$. Throughout the data analysis, corrections were made for instrumental smearing. The parameters in the analysis were optimized by means of a nonlinear least-square fitting program and the errors on the parameters were calculated by the standard method [38].

3.2. Dynamic light scattering

The signal generated by the light scattering from diffusing particles can be analyzed by its intensity autocorrelation function $G^I(\tau)$ [39]

$$G^I(\tau) = \langle I(t) I(t+\tau)\rangle \tag{9}$$

where $I(t)$ is the scattered light intensity at time t and $I(t+\tau)$ is the scattered light intensity at some later time $(t+\tau)$. The normalized intensity autocorrelation function $g^I(\tau)$ is

$$g^I(\tau) = \frac{G^I(\tau)}{\langle I(t)\rangle^2} \tag{10}$$

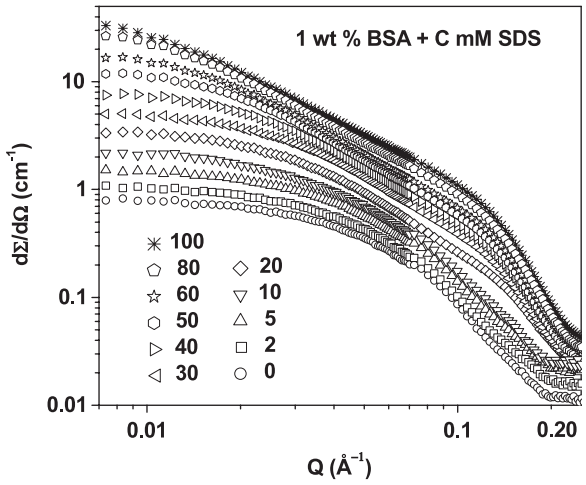

Figure 1. SANS data for 1 wt% BSA with varying SDS concentration.

The electric field autocorrelation function $g^E(\tau)$ is related to the normalized intensity autocorrelation function by

$$g^I(\tau) = 1 + B[g^E(\tau)]^2 \tag{11}$$

where B is an experimental parameter which mainly depends on the detection optics and alignment. For a mono-disperse system of particles, $g^E(\tau)$ follows a simple exponential decay with decay constant γ:

$$g^E(\tau) = \exp[-\gamma\tau] \tag{12}$$

The average decay rate (γ) of $g^E(\tau)$ has been estimated using a monomodal fit. The apparent diffusion coefficient (D_a) is obtained from the relation $\gamma = D_a Q^2$ and the corresponding effective hydrodynamic size calculated using the Stoke–Einstein relationship.

4. Results and discussion

SANS data for 1 wt% BSA in the presence of varying SDS concentrations are shown in figure 1. These data do not show any correlation peak, which is characteristic of interacting charge colloids [40]. This is a consequence of an appropriate choice of pH and ionic strength of the solutions and component concentrations to match the condition where the system can be treated as a dilute solution (i.e. $S_p(Q) \sim 1$). Based on the features of the scattering profiles, the data can be grouped in two different sets as the surfactant concentration is increased. The first data set corresponds to proteins at low surfactant concentrations (0–10 mM), where the scattering data show similar behavior to that of pure protein solution. In this data set, the overall scattering cross-section increases with an increase in surfactant concentration. It can be explained in terms of equation (1) if the individual surfactant molecules bind to protein and the volume of the scattering particle increases. The features of the scattering data in the second data set at higher surfactant concentrations (>10 mM) are very different to those of the first data set. One of the interesting features is the linearity of the scattering profiles on a log–log scale in the intermediate Q range, with a Q range of linearity increasing with surfactant concentration. This is an indication of the formation of a fractal structure by the protein–surfactant complex [23–25]. The build-up of scattering cross-section in the higher cut-off of

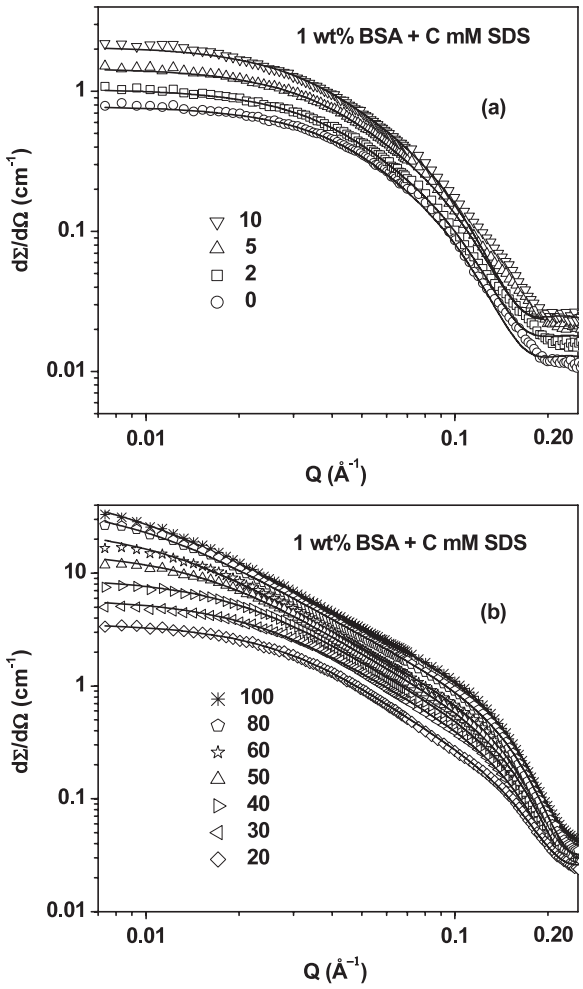

Figure 2. SANS data for 1 wt% BSA with (a) low SDS concentrations 0–10 mM and (b) higher SDS concentrations 20–100 mM. Points represent the experimental data and the solid lines are the theoretical fits to the data.

the linearity of scattering data suggests the formation of surfactant aggregates, and the lower cut-off corresponds to the overall size of the protein–surfactant complex. It is observed that the position of high-Q cut-off remains almost the same, while the position of low-Q cut-off shifts to smaller Q values with increasing surfactant concentration. The fitted data using detailed analysis are shown in figure 2.

The fitted SANS curves for the first data set of figure 1 using equation (1) are shown in figure 2(a). The calculated structural parameters in this system are given in table 1. It is found that, in a pure protein solution, the protein macromolecules have a prolate ellipsoidal shape with semi-major and semi-minor axes as 70.2 and 22.2 Å, respectively. This result is in good agreement to those reported earlier [24, 25]. In the first data set, the protein macromolecules maintain their folded structure on the addition of surfactant. It is believed that individual surfactant molecules bind to the proteins at low surfactant concentrations [6]. The data are fitted considering that all of the surfactant molecules are bound to the protein,

Table 1. Fitted parameters of SANS analysis of protein–surfactant complex for 1 wt% BSA with low SDS concentrations 0–10 mM. Data are fitted for prolate ellipsoidal shape ($a \neq b = c$) of the protein macromolecule.

[SDS] (mM)	Semi-major axis, a (Å)	Semi-minor axis, $b = c$ (Å)
0	70.2 ± 5.1	22.2 ± 0.8
2	77.3 ± 5.8	22.2 ± 0.8
5	80.0 ± 6.1	22.2 ± 0.8
10	88.0 ± 6.4	23.0 ± 0.9

Table 2. Fitted parameters of SANS analysis of protein–surfactant complex for 1 wt% BSA with higher SDS concentrations 20–100 mM. Data are fitted for a fractal structure of micelle-like clusters randomly distributed along the unfolded protein chain.

[SDS] (mM)	Fractal dimension, D	Correlation length, ξ (Å)	Micelle radius, R (Å)	Number of micelles, N	Aggregation number, n
20	2.27 ± 0.15	38.0 ± 1.9	18.0 ± 0.6	2	51
30	2.15 ± 0.14	43.0 ± 2.7	18.0 ± 0.6	3	50
40	2.05 ± 0.13	54.0 ± 3.8	18.0 ± 0.6	4	50
50	1.95 ± 0.10	67.8 ± 4.9	18.0 ± 0.6	6	45
60	1.88 ± 0.09	87.9 ± 5.4	18.0 ± 0.6	8	43
80	1.79 ± 0.06	117.9 ± 6.9	18.0 ± 0.6	10	42
100	1.71 ± 0.04	144.3 ± 7.5	18.0 ± 0.6	13	42

as it is known that only a very small fraction of surfactant molecules in the protein–surfactant system are adsorbed at the air–water interface or remain free [32]. Table 1 shows changes in the dimensions of the protein on increasing binding of surfactant molecules as a function of surfactant concentration. The semi-minor axis remains almost the same, while the semi-major axis increases with increasing surfactant concentration. The size of the protein elongates from 70 to 88 Å along the semi-major axis on the addition of 10 mM of surfactant. Similar results of the elongation of the BSA protein have also been observed with the cationic surfactant azobenzene trimethyl ammonium bromide. It is believed that the six protein sub-domains forming BSA remain intact but separate from each other, leading to an elongation of the protein on the addition of surfactant [41].

Based on the linearity of the scattering data on a log–log scale, the second data set in figure 1 has been fitted using a fractal structure (equation (6)) of protein–surfactant complex. The fitted data are shown in figure 2(b). The fractal structure of the complex on the basis of the necklace model considers micelle-like clusters of the surfactant formed along the unfolded polypeptide chain of the protein. The slope of the scattering data on a log–log scale gives the value of the fractal dimension D of the complex. The cut-offs of the linear range of the data at low and high Q value are, respectively, related to the formation of the extent of the complex and the size of the individual micelles in the complex [37]. It is believed that the increase in surfactant concentration as well as all the bound surfactant molecules of the first set participates in the formation of micelle-like clusters [32]. The fitted parameters of the analysis are given in table 2. It is found that the fractal dimension decreases and the overall size of the complex increases on increasing the surfactant concentration. The size of micelle-like clusters (R) does not change, while the number of such micelle-like clusters (N) in a protein–surfactant complex increases with the surfactant concentration (table 2). The calculated aggregation number of micelle-like clusters (n) in the complex decreases from 51 to 42 on increasing the surfactant concentration from 20 to 100 mM. It is interesting to note that these values of aggregation

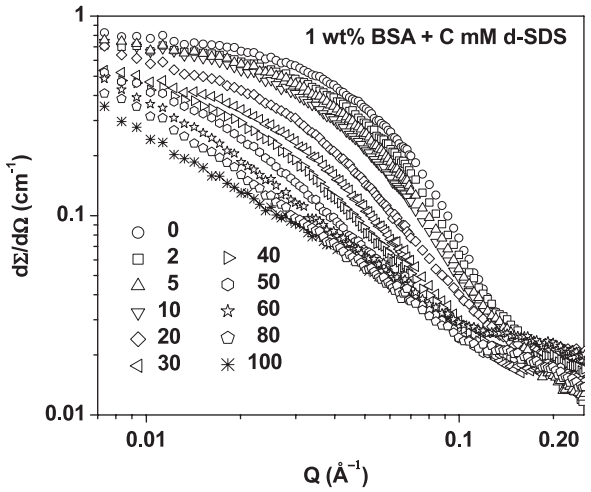

Figure 3. SANS data for 1 wt% BSA with varying d-SDS concentration.

numbers are much smaller than what one would have found (about 70) in pure surfactant solution for a similar size of micelle [42]. This indicates the participation of the hydrophobic portions of the unfolded protein chain in micellar formation [25, 32]. The participation of the unfolded protein in the formation of micelle-like clusters is enhanced with the increase in unfolding, and this results in a decreasing aggregation number of micelle-like clusters [36]. Also, all the surfactant molecules probably participate in the micelle-like clusters to avoid the exposure of hydrophobic portions of the protein on its unfolding with an increase in surfactant concentration.

The conformational changes of protein in a protein–surfactant complex have been examined by contrast variation SANS by contrast matching the surfactant. The surfactant is contrast matched using deuterated SDS (d-SDS) and the sample is prepared in D_2O. Figure 3 shows the SANS data for 1 wt% BSA in the presence of varying d-SDS concentration. Unlike in figure 1, where the scattering cross-section increases on increasing SDS concentration, figure 3 shows a decrease in scattering cross-section with an increase in d-SDS concentration. This can be understood in terms of equation (1) that the contrast of protein decreases as the size of the complex increases on the addition of surfactant (tables 1 and 2). Similar to figure 1, figure 3 also shows two sets of data as obtained: the first set at low surfactant concentration and the second set at high surfactant concentration. The first data set corresponds to the binding of individual surfactant molecules and hence the size of the complex increases as more and more surfactant is added (table 1). This data set is fitted with equation (1) and shown in figure 4(a). The analysis of the data (table 3) gives similar dimensions of the complex as obtained in table 1. This is also clearly visible in the nice overlap of normalized corresponding data, for example for 1 wt% BSA with 5 mM SDS and d-SDS, as shown in the inset of figure 4(a). The overlap suggests that surfactant molecules bind uniformly and therefore, by contrast matching surfactant, only the contrast of the complex decreases [43]. The fitted data of the second set are shown in figure 4(b). In these systems micelle-like clusters of surfactant molecules are formed in the complex (table 2). This non-uniform distribution of surfactant in the complex is also verified from the fact that the scattering curves of protein with SDS and d-SDS cannot be scaled on top of each other (inset of figure 4(b)) in contrast to the case before, where the surfactant is uniformly distributed in the complex (inset of figure 4(a)). The unfolded protein in the complex is fitted by the scattering function obeying random coil Gaussian conformation as [44]

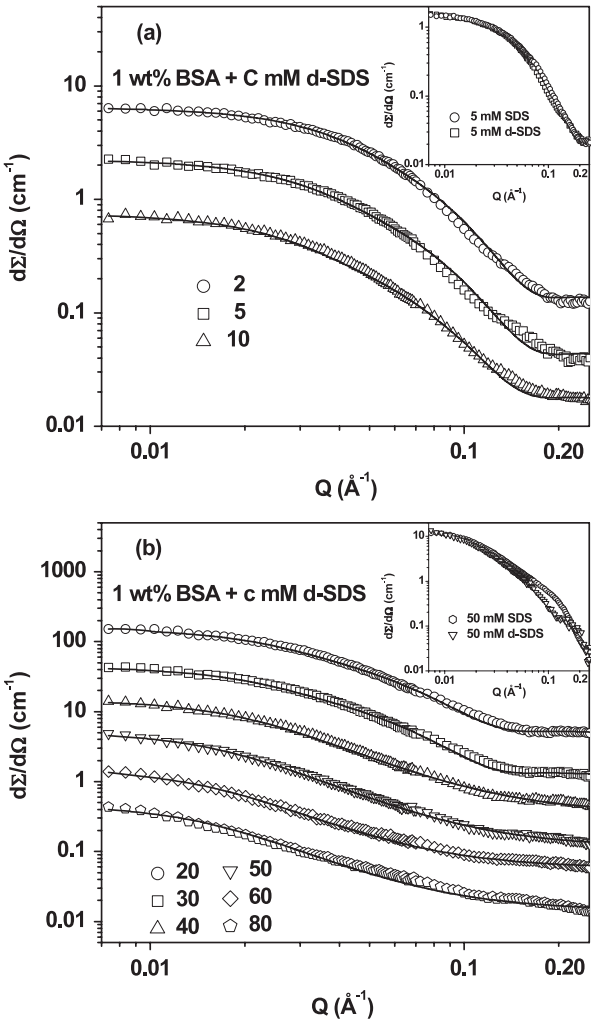

Figure 4. SANS data for 1 wt% BSA with (a) low d-SDS concentrations 0–10 mM and (b) higher d-SDS concentrations 20–80 mM. Points represent the experimental data and the solid lines are the theoretical fits to the data. The insets show, on a normalized scale, the differences between complexes including SDS and d-SDS.

Table 3. Fitted parameters of SANS analysis of protein–surfactant complex for 1 wt% BSA with varying d-SDS concentration. Data are fitted as a prolate ellipsoidal shape for the folded protein structure and a random Gaussian coil for the unfolded protein structure.

[d-SDS]	Folded structure		Unfolded structure
(mM)	Semi-major axis, a (Å)	Semi-minor axis, $b = c$ (Å)	Radius of gyration, R_g (Å)
0	71.0 ± 5.1	22.2 ± 0.8	—
2	77.3 ± 5.8	22.2 ± 0.8	—
5	82.0 ± 6.3	22.2 ± 0.8	—
10	88.0 ± 6.4	23.0 ± 0.9	—
20	94.0 ± 6.7	25.8 ± 1.1	—
30	99.0 ± 7.1	27.1 ± 1.3	—
40	—	—	60.1 ± 1.6
50	—	—	70.3 ± 1.8
60	—	—	85.5 ± 2.4
80	—	—	102.3 ± 4.6

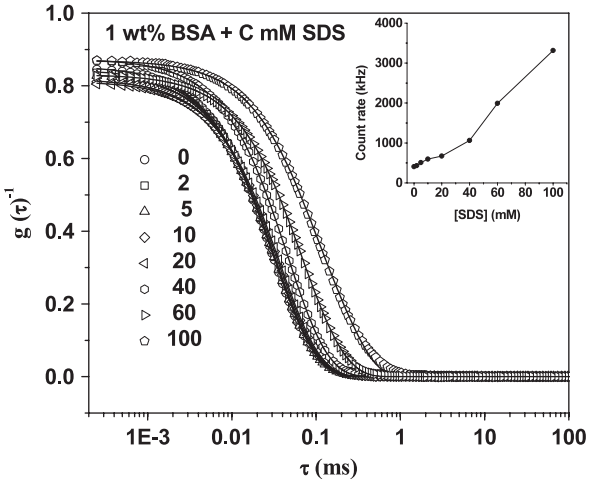

Figure 5. DLS data for 1 wt% BSA with varying SDS concentration. The inset shows the corresponding variation of the average count rate measured at the detector with an increase in surfactant concentration.

Table 4. Fitted parameters as obtained by DLS for the protein–surfactant complex with 1 wt% BSA and varying SDS concentrations. SANS results are compared with the effective size of protein–surfactant complex calculated from table 1 as $(ab^2)^{1/3}$ for the folded structure and, from table 2, as ξ for the unfolded structure.

[SDS] (mM)	Diffusion coefficient, D_a (10^{-8} cm^2 s^{-1})	Hydrodynamic radius, R_h (Å)	SANS effective size, R_e (Å)
0	64.3	33.5	32.6
2	64.3	33.5	33.5
5	59.0	36.5	34.1
10	55.2	39.0	36.0
20	51.9	41.5	38.0
40	35.7	60.3	54.0
60	23.6	91.2	87.9
100	14.3	150.5	144.3

$$\frac{d\Sigma}{d\Omega}(Q) \sim (QR_g)^{-4}\left[Q^2R_g^2 - 1 + \exp(-Q^2R_g^2)\right], \tag{13}$$

where R_g is the radius of gyration of the unfolded protein chain. The value of R_g increases on the addition of surfactant (table 3). It may be mentioned that at d-SDS concentration of 20 and 30 mM, where the complex already consists of micelle-like clusters, the data are still best fitted with a prolate ellipsoidal shape of the protein. Unfolding in these systems is limited due to the formation of a small number of micelles in the complex (table 2).

DLS data for 1 wt% BSA on the addition of surfactant are shown in figure 5. In DLS, time-dependent fluctuations in the intensity of scattered light are measured [39]. These fluctuations happen as a result of the Brownian motion, arising from the particles undergoing random collisions. Small particles diffuse rapidly and yield fast fluctuations, whereas large particles and aggregates generate relatively slow fluctuations. The rate of the fluctuations can be determined through the technique of autocorrelation analysis. The analysis of intensity fluctuations enables determination of the diffusion coefficient, which then can be converted to a size using the

Stoke–Einstein relationship. Figure 5 shows the slowing down of the intensity auto correlation function with increasing surfactant concentration. The analysis suggests that, irrespective of the surfactant concentration, all the data fit to the single diffusion coefficient (equation (12)) for the structure of the protein–surfactant complex. The fitted values of the apparent diffusion coefficient (D_a) and the corresponding hydrodynamic radius (R_h) are given in table 4. There is a decrease in the value of D_a and an increase in R_h with an increase in surfactant concentration. The diffusion coefficient decreases as the amount of surfactant in the complex increases, either through the binding of surfactant molecules as individuals or through the formation of micelle-like clusters with the protein. This is consistent with the average count rate measured at the detector, which increases with the increase in the surfactant concentration (inset of figure 5). The increase in the overall size of the complex is significant at higher surfactant concentrations, as related to the unfolding of protein. These observations are in agreement with the results obtained using SANS. The larger values of the sizes of the complex obtained using DLS rather than SANS (table 4) are expected, because DLS measures structure along with its hydration.

5. Conclusions

SANS and DLS studies have been used to examine the structural changes in the protein BSA on the addition of varying concentrations of the surfactant SDS. It is found that the binding of ionic surfactant molecules to the protein disrupts the native structure of the protein. Two interesting regions of surfactant concentration are associated with structural formation of the surfactant with the protein. The first one at low surfactant concentrations is related to the binding that occurs at specific sites through electrostatic interaction. The second one is obtained at higher surfactant concentrations where a large increase in binding due to cooperative surfactant interaction results in unfolding of the protein. At lower surfactant concentrations, the increase in the dimensions of the ellipsoidal protein due to surfactant binding has been determined. The results show that the semi-minor axis remains more or less constant and the changes occur mostly along the semi-major axis. At higher surfactant concentrations, the SANS data suggests the formation of micelle-like clusters in the complex. It has been found that the size of the micelle-like clusters does not change and unfolding of the protein occurs due to the increase in the number of such micelles in the complex with surfactant concentration. The radius of gyration of the unfolded protein, as measured by contrast-matched surfactant, increases with surfactant concentration.

Acknowledgments

The authors wish to thank Dr F Pfeiffer and M Dierolf for their kind help during the DLS experiments. This work is based on SANS experiments performed at the Swiss Spallation Neutron Source SINQ, Paul Scherrer Institut, Villigen, Switzerland.

References

[1] McClements D J 2004 *Curr. Opin. Colloid Interface Sci.* **9** 305
[2] Dickinson E 2006 *Soft Matter* **2** 642
[3] Goddard E D and Ananthapadmanabhan K P 1993 *Interactions of Surfactants with Polymers and Proteins* (London: CRC Press)
[4] Sun C, Yang J, Wu X, Huang X, Wang F and Liu S 2005 *Biophys. J.* **88** 3518
[5] De S, Girigoswami A and Das S 2005 *J. Colloid Interface Sci.* **285** 562
[6] Jones M N 1992 *Chem. Soc. Rev.* **21** 127
[7] Morén A K and Khan A 1998 *Langmuir* **14** 6818
[8] Morén A K, Nydén M, Söderman O and Khan A 1999 *Langmuir* **15** 5480
[9] Stenstam A, Khan A and Wennerström H 2001 *Langmuir* **17** 7513

[10] Reynolds J A and Tanford C 1970 *J. Biol. Chem.* **245** 5161
[11] Valstar A, Brown W and Almgren M 1999 *Langmuir* **15** 2366
[12] Otzen D E 2002 *Biophys. J.* **83** 2219
[13] Mackie A and Wilde P 2005 *Adv. Colloid Interface Sci.* **117** 3
[14] Chakraborty A, Seth D, Setua P and Sarkar N 2006 *J. Phys. Chem.* B **110** 16607
[15] Vasilescu M, Angelescu D, Almgren M and Valstar A 1999 *Langmuir* **15** 2635
[16] Valstar A, Almgren M, Brown W and Vasilescu M 2000 *Langmuir* **16** 922
[17] Stenstam A, Khan A and Wennerström H 2004 *Langmuir* **20** 7760
[18] Deep S and Ahluwalia J C 2001 *Phys. Chem. Chem. Phys.* **3** 4583
[19] Xu Q and Keiderling T A 2004 *Protein Sci.* **13** 2949
[20] Stenstam A, Topgaard D and Wennerström H 2003 *J. Phys. Chem.* B **107** 7987
[21] Jones M N, Skinner H A and Tipping E 1975 *Biochem. J.* **147** 229
[22] Gimel J C and Brown W 1996 *J. Chem. Phys.* **104** 8112
[23] Chen S H and Teixeira J 1986 *Phys. Rev. Lett.* **57** 2583
[24] Guo X H and Chen S H 1990 *Phys. Rev. Lett.* **64** 1979
[25] Seth E and Aswal V K 2003 *J. Macromol. Sci. Phys.* B **42** 85
[26] Shinagawa S, Sato M, Kameyama K and Takagi T 1994 *Langmuir* **10** 1690
[27] Santos S F, Zanette D, Fischer H and Itri R 2003 *J. Colloid Interface Sci.* **262** 400
[28] Gelamo E L, Itri R, Alonso A, Silva J V D and Tabak M 2004 *J. Colloid Interface Sci.* **277** 471
[29] Shweitzer B, Zanette D and Itri R 2004 *J. Colloid Interface Sci.* **277** 285
[30] Jones M N and Chapman D 1995 *Micelles, Monolayers and Biomembranes* (New York: Wiley–Riss)
[31] Shirahama K, Tsujii K and Takagi T 1974 *J. Biochem. (Tokyo)* **75** 309
[32] Turro N J, Lei X G, Ananthapadmanabhan K P and Aronson M 1995 *Langmuir* **11** 2525
[33] Kohlbrecher J and Wagner W 2000 *J. Appl. Crystallogr.* **33** 804
[34] Wignall G D and Bates F S 1987 *J. Appl. Crystallogr.* **20** 28
[35] Hayter J B and Penfold J 1983 *Colloid Polym. Sci.* **261** 1022
[36] Guo X H, Zhao N M, Chen S H and Teixeira J 1990 *Biopolymers* **29** 335
[37] Teixeira J 1988 *J. Appl. Crystallogr.* **21** 781
[38] Bevington P R 1969 *Data Reduction and Error Analysis for Physical Sciences* (New York: McGraw-Hill)
[39] Pecora R 1985 *Dynamic Light Scattering* (New York: Plenum)
[40] Chen S H, Sheu E Y, Kalus J and Hoffmann H 1988 *J. Appl. Crystallogr.* **21** 751
[41] Lee T C, Smith K A and Hatton A T 2005 *Biochemistry* **44** 524
[42] Aswal V K and Goyal P S 2003 *Phys. Rev.* E **67** 051401
[43] Ganguly R, Aswal V K, Hassan P A, Gopalkrishnan and Kulshreshtha S K 2006 *J. Phys. Chem.* B **110** 9843
[44] Debye P 1947 *J. Phys. Coll. Chem.* **51** 18